

# We are IntechOpen, the world's leading publisher of Open Access books Built by scientists, for scientists

6,900

Open access books available

186,000

International authors and editors

200M

Downloads

Our authors are among the

154

Countries delivered to

TOP 1%

most cited scientists

12.2%

Contributors from top 500 universities



WEB OF SCIENCE™

Selection of our books indexed in the Book Citation Index  
in Web of Science™ Core Collection (BKCI)

Interested in publishing with us?  
Contact [book.department@intechopen.com](mailto:book.department@intechopen.com)

Numbers displayed above are based on latest data collected.  
For more information visit [www.intechopen.com](http://www.intechopen.com)



---

# Polyolefine Composites Reinforced by Rice Husk and Saw Dust

---

Thi Thu Loan Doan, Hanna M. Brodowsky and  
Edith Mäder

Additional information is available at the end of the chapter

<http://dx.doi.org/10.5772/65264>

---

## Abstract

Due to the global demand for fibrous light-weight materials, research on composites reinforced with plant materials has increased. Natural fiber reinforced composites offer several advantages: light weight, competitive specific mechanical properties, easy processing, large volume availability, low cost, and low environmental footprint. Especially, using agricultural wastes such as rice husk, saw dust etc. as fillers/fibres in composites provides the chance to improve material properties while improving their sustainability. In the present work, rice husk and saw dust were chosen as fillers for their differing morphology, aspect ratios, and difference of structure. As matrices, polyethylene (PE) and polypropylene (PP) were studied, either neat or modified with maleic anhydride grafted PP/PE as coupling agent or compatibilizer between hydrophobic matrices and hydrophilic bio-fillers. The bending modulus is improved due to filler addition. In presence of compatibilizer, the improved interfacial interaction leads to improved bending and tensile strength as well as toughness. Furthermore, the influence of the filler and compatibilizer on composite properties such as hardness, dynamic mechanical behaviour, thermal expansion, thermal degradation, melting and crystallisation behaviour are presented.

**Keywords:** natural fibers, bio-fillers, composites, interphase

---

## 1. Introduction

The global demand for light-weight materials calls for the broad use of fiber-reinforced plastic materials [1]. Developing composites using natural fibers provides the chance to improve

materials while decreasing their ecological footprint. Even using agricultural and forestry wastes such as rice husks (RHs), coconut fibers, bagasse, and saw dust (SD) can lead to significantly improved material properties [2].

Rice husk and saw dust, by-products of the rice milling and wood sawing processes respectively, are potential reinforcing fillers for thermoplastic matrix composites because of their lignocellulosic characteristics. These fillers offer advantages of easy processing, large volume availability, annual renewability, low cost, light weight, competitive specific mechanical properties, and high sustainability. The morphology differs: Rice husk is made up of rectangular platelets and saw dust of short fiber bundles.

The most common thermoplastics used as matrices for bio-fillers are polyethylene (PE) and polypropylene (PP). When a polyolefin is used as a matrix for a bio-filler composite, the incompatibility between hydrophobic matrix and hydrophilic bio-filler is an important issue. Therefore, there have been many studies on improving interfacial interactions between the polymers and bio-fillers. According to previous studies, the best solution of the problem is using an appropriate coupling agent or compatibilizer such as maleic anhydride-functionalized polyolefin, for example, maleic anhydride-grafted polypropylene (MAPP) for PP or maleic anhydride-grafted polyethylene (MAPE) for PE [3–8].

Biomaterials such as saw dust, bamboo powder, or grain husks used as fillers in polymer matrix composites are natural compounds, mainly containing cellulose, hemicellulose, and lignin. Their degradation takes place at a relatively low temperature, around 200°C [1]. Therefore, bio-fillers will be subjected to thermal degradation during composite processing with the majority of common thermoplastic polymers [2]. This leads to undesirable properties, such as odor and browning along with a reduction in mechanical properties of the bio-composite [2, 3]. Therefore, it is important to understand and predict the thermal decomposition processes of bio-filler in order to better design composite processes and estimate the influence of the thermal decomposition on composite properties [4].

In this work, the suitability of rice husk and saw dust as reinforcing agents for composites based on different polyolefine matrices was evaluated. The filler morphology is characterized. Mechanical tests of their composites were evaluated as a function of filler content and filler morphology. The effect of maleated polyolefines as compatibilizers on the mechanical properties of the composites as well as hardness of the composites was studied.

Thermal studies of biomaterial-filled polyolefine (PP, PE) composites included thermomechanical analysis (TMA) and the thermal and mechanical dynamic behavior according to the filler loading and the presence of compatibilizers. The crystallization is characterized by differential scanning calorimetry (DSC) analysis and the thermal degradation by thermogravimetric analysis (TGA).

## 2. Experimental

### 2.1. Materials

Polypropylene, Advanced PP-1100N, and high-density polyethylene, EL-Lene H5818J, were supplied by Advanced Petrochemical Co. and SCG Plastics Co., Ltd, Thailand, respectively. Two compatibilizers, maleic anhydride-grafted polypropylene Polybond 3200 and maleic anhydride-grafted polyethylene Polybond 3029, were provided by Chemtura, USA. **Table 1** shows the typical physical properties of the matrix polymers and compatibilizers.

Polymers properties	PP	PE	MAPP	MAPE
Density (g/cm <sup>3</sup> )	0.91	0.96	0.91	0.96
Melting point (°C)	163	131	157	130
Melt flow index (g/10 min)	12*	18**	115*	
MA content (%)	–	–	1.0	1.6
Tensile strength (MPa)	35.0	28.0	–	–
Notched Izod impact strength (kJ/m <sup>2</sup> )	3.0	4.8	–	–

\*MFI at 230°C/2.16 kg

\*\*MFI at 190°C/2.16 kg

**Table 1.** Properties of studied polymer materials.

Rice husk obtained from a rice mill factory in Danang, Vietnam, was ground. Saw dust from *Acacia auriculiformis* tree was collected from a Wood processing factory in Danang, Vietnam. Rice husk and saw dust were screened and dried at 80°C for 24 h before preparing the composites. Where a wood block was used for comparison, its dimensions were the same as those of the composite samples in the tests.

### 2.2. Methods

#### 2.2.1. Aspect ratio of fillers

A digital microscope (Keyence VHX-100, Japan) and the corresponding imaging system were used for the aspect ratio determination. About 500-mg fillers of each filler type, classified by the sieve opening, were placed on a glass dish under the microscope. The optical light was adjusted to achieve the best focusing alignment and image resolution. The filler images taken with a digital camera were used to measure the length and diameter of individual filler particles. A minimum of 100 filler particles were measured for each sample. The aspect ratio was described as the ratio of length and width of the fibrous wood and as length and width of the rice husk platelets. Note the latter were not characterized by the length-to-plate-thickness ratio.

### 2.2.2. Particle size distribution of fillers

To evaluate the particle size distribution, fillers were classified after grinding (for rice husk) by screening into four mesh size ranges 20–35, 35–45, 45–80, and >80 per inch (approximately 500–850, 350–500, 180–350  $\mu\text{m}$ , and <180  $\mu\text{m}$ ). The filler particles were then weighed in order to determine the weight of the fillers in each mesh size range.

### 2.2.3. Preparation of the composites

Composites were produced in a two-stage process. In the first stage, bio-fillers and polyolefine were compounded with and without compatibilizer using the twin-screw extruder Rheomex CEW100 QC, Haake, Germany. The mixing zone temperature of the extruder was 160°C for PE and 190°C for PP matrix composites. The rotation speed of the screws was 50 rpm. In the second stage, the extrudate in the form of strands was cooled to room temperature and then granulated.

The compound granules were dried at 80°C for 24 h before injection molding. The specimens were prepared using the injection molding machine MiniJet II, Haake, Germany, at cylinder temperatures of 180°C for PE and 190°C for PP matrix composites under an injection pressure of 800 bar.

### 2.2.4. Mechanical testing

Tensile and bending tests were conducted with the Universal Testing Machine AG-X plus, Shimadzu, Japan, according to ISO 527-3 and ISO 178, respectively. Notched Izod impact tests were conducted with HIT 50P, Zwick/Roell, Germany, according to ISO 180 at room temperature. Each value obtained represents the average of at least five samples.

### 2.2.5. Hardness tests

The hardness determination of the composites was carried out according to ISO 2039-1 on specimens of 80 mm  $\times$  10 mm  $\times$  4 mm. The specimens were loaded using the force of 132.39 N for a duration of 30 s. Each value obtained represents the average of 10 positions of measurement.

### 2.2.6. SEM analysis

Studies on the morphology of fillers and the tensile fracture surfaces of the composites were carried out using a FE-SEM (Ultra 55, Carl Zeiss SMT AG, Germany).

### 2.2.7. Thermomechanical analysis (TMA)

The thermal expansion tests of the composites and pure polyolefine samples were conducted using a thermomechanical analyzer (TMA Q400 V7.4 Build 93, TA Instruments) from –10 to 100°C at a heating rate of 2°C/min in a nitrogen atmosphere. The expansion mode with a constant compression load of 0.02 N was used on specimen of 5 mm  $\times$  5 mm  $\times$  4 mm.

### 2.2.8. Dynamic mechanical thermal analysis (DMTA)

Dynamic mechanical thermal analysis was carried out (DMA Q800 V20.24 Build 43, TA Instruments) in N<sub>2</sub> atmosphere. The dimensions of the test specimens were 17.5 mm × 10 mm × 4 mm. The tests were performed using a three-point bending-rectangular measuring system at 1-Hz test frequency. The heating rate was 1 K/min in the temperature range of -50 to 150°C. E' (storage modulus), E'' (loss modulus), and Tan δ (damping peak) of the samples were determined as a function of temperature.

### 2.2.9. Differential scanning calorimetry (DSC)

The samples used for the differential scanning calorimetric analysis were cut from extruded pellets. Approximately 10 mg of each sample was used. The equipment (DSC Q2000 V24.10 Build 122, TA Instruments) was programmed to work at the temperature range between 0 and 250°C, under a nitrogen flow of 50 mL/min. The heating and cooling rates were 10 K/min.

The values of melting temperature ( $T_m$ ) and the melting enthalpy ( $\Delta H_m$ ) were calculated from the second heating. The crystallization temperature ( $T_c$ ) was calculated from the cooling cycle.

### 2.2.10. Thermogravimetric analysis (TGA)

The samples used for the thermogravimetric analysis were cut from extruded pellets. Approximately 10 mg of each sample was used. The thermogravimetric analysis (TGA Q500 V6.7 Build 203) was carried out under nitrogen and air atmospheres in a temperature range of 23–700°C. The heating rate of the analysis was 10 K/min.

## 3. Results and discussion

### 3.1. Characterization of the fillers

Filler particle size and shape are important factors for reinforcement materials. **Figure 1** shows selected SEM images of RH and SD fillers. The morphologies differ strongly: SD is made up of lengthwise agglomerated fibers, whereas RH is made up of platelets with protrusions aligned in a regular pattern (**Figures 1b, d** and **2**). Detailed analysis shows a hollow cellular structure in both fillers (**Figure 1c, d**). The milling leads to different modes of fracture: In saw dust, the fibers separate, partially branch off or break, sometimes the cells collapse or the cell walls open, resulting in a highly nonuniform morphology with an irregular surface, which will allow to interact with the molten polyolefine during compounding and increase the chance of mechanical interlocking. In contrast, in RH the platelets have a highly regular pattern of 30 μm protrusions in a 90° array on the outside and a smooth inside. In the detailed image (**Figure 2a**), additional hair-like structures become visible between the protrusions. Platelet fracture occurs mainly along the lines between the protrusions, leading to platelets of angular shape and of rather uniform thickness (50 μm), and the cellular structure is contained within the platelet.

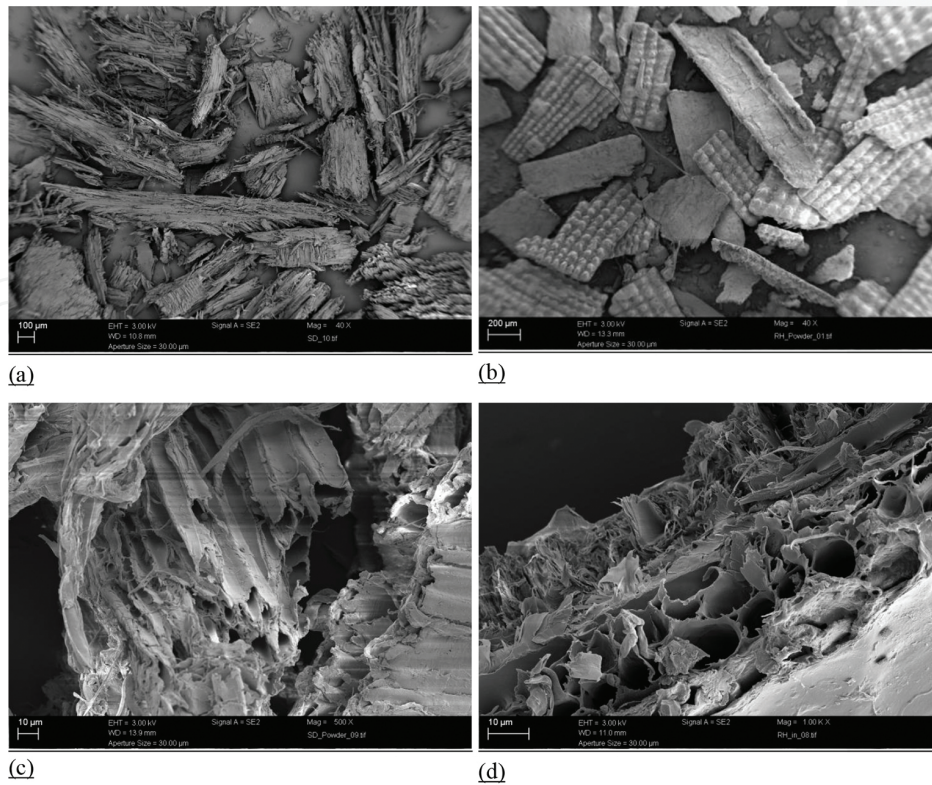


**Figure 1.** SEM micrographs of the fillers: surface morphology of (a, c) saw dust and (b, d) rice husk.

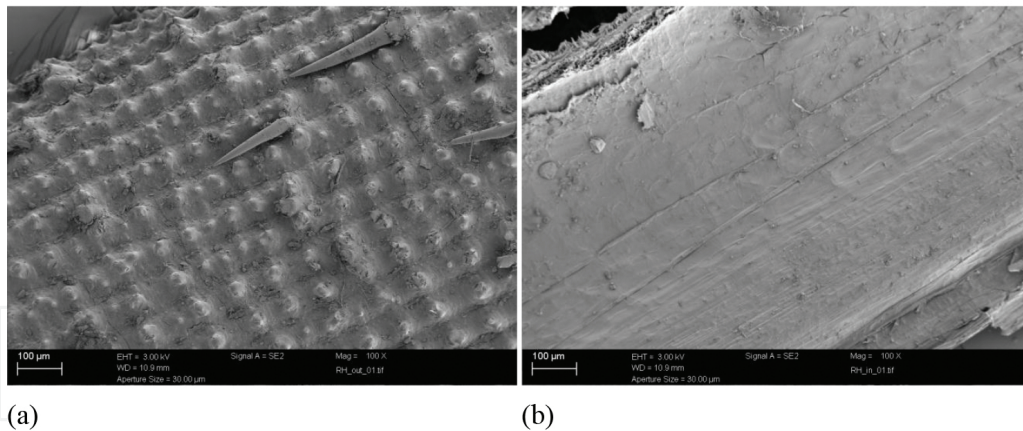


**Figure 2.** SEM micrographs of the morphology of rice husk (a) outer and (b) inner surface.

The filler surface layer plays an important role in surface tension and thus in wettability. It has been postulated that the inner RH surface contains lipid and proteinaceous compounds bound to the protein molecule by ester or thioester bonds [9]. The amount of lipid on the filler surface has an influence on hydrophobicity and surface tension.

**Figure 3** shows particle size distribution and aspect ratio of the rice husk and saw dust fillers. About 80% of RH and SD fillers were in the range of 180–500 µm. The aspect ratio of both saw

dust and rice husk fillers is quite small. The fibrous saw dust has a higher aspect ratio in the range of 4–5 compared to rice husk filler formed of rectangular platelets with an aspect ratio of 2–3. Note that for better comparison, length-to-width ratio is used for both filler types. The commonly used aspect ratio for platelets—diameter to thickness—scales with the particle size as the thickness is around 50  $\mu\text{m}$  for all platelets.

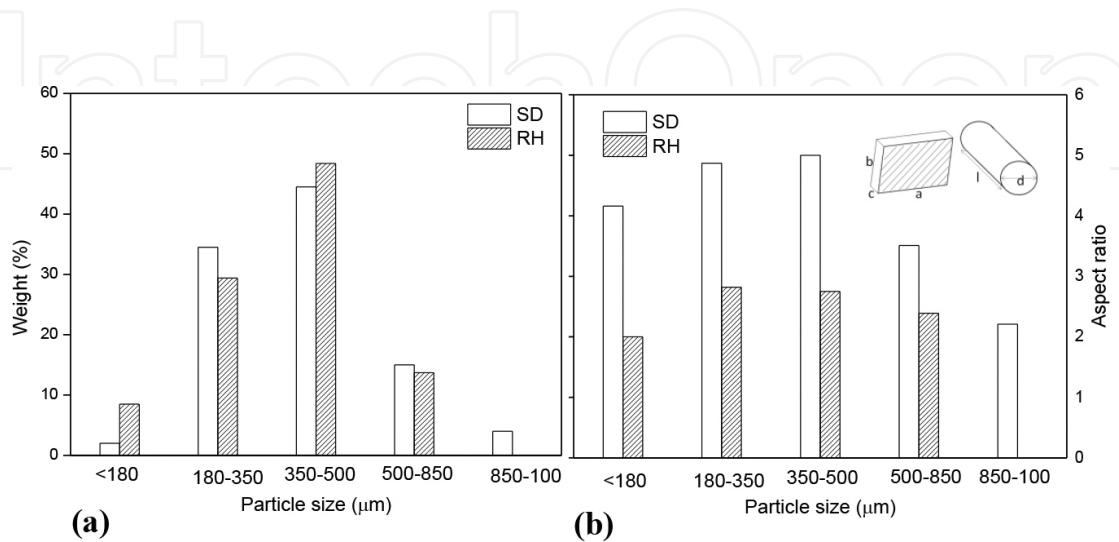


**Figure 3.** Size distribution (a) and aspect ratio (b) of filler particles (saw dust SD and rice husk RH). inset: Model of filler shape: platelets ( $a \times b \times c$ ) for rice husk, circular rods (length  $l$ , diameter  $d$ ) for saw dust. Note: Here calculation of aspect ratio is  $l/d$  for a rod and  $a/b$  for platelets.

A simple model is used to estimate the surface area of the particles, cf. **Figure 3b** inset: RH platelets may be modeled as rectangular blocks of 50  $\mu\text{m}$  thickness and SD as spherical rods. The surface-to-volume ratio of a thin platelet is dominated by thickness (or,  $2/\text{side length } a + 2/\text{side length } b + 2/\text{thickness}$ ), whereas that of a long circular rod is roughly proportional to the inverse of the diameter ( $4/\text{diameter} + d/\text{rod length}$ ). A rough estimate of the surface area per volume (with a size distribution and aspect ratio as shown in **Figure 3** and considering the densities of 1.3  $\text{g}/\text{cm}^3$  for SD and 1.5  $\text{g}/\text{cm}^3$  for RH) shows that in a given weight, RH contains a factor of two higher number of particles, but the filler surface area vs. particle size distribution is only slightly shifted to smaller particle sizes in SD. The total filler surface area of the two filler types is equal according to this simple model.

### 3.2. Mechanical properties of the composites

The good specific mechanical properties are the prime reason for the application of filled polymer composites. The mechanical properties of the filler/polymer composites depend strongly on filler loading, interfacial adhesion, the degree of dispersion, and the filler particle size [10, 11]. **Figures 4, 5, and 6a** show the effects of filler content on the mechanical properties of bio-filler/polyolefine composites. The stated filler content is the wt.%, with a density of 1.3  $\text{g}/\text{cm}^3$  for SD and 1.5  $\text{g}/\text{cm}^3$  for RH, and the volume contents are approximately 4% lower for SD and 7% lower for RH.

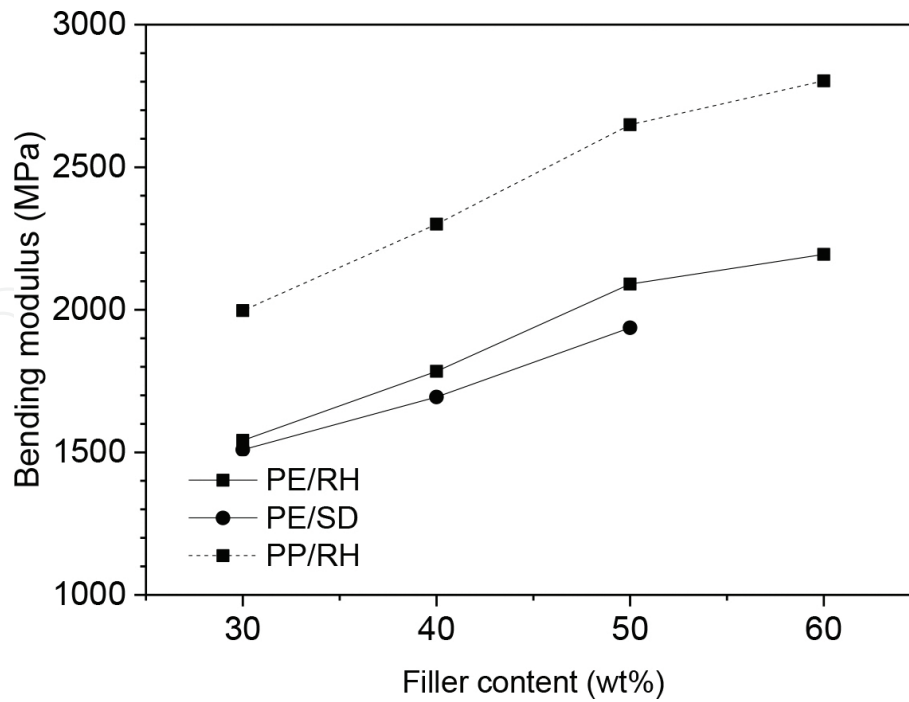


**Figure 4.** Influence of filler content on bending modulus of the three composites, no compatibilizer added.

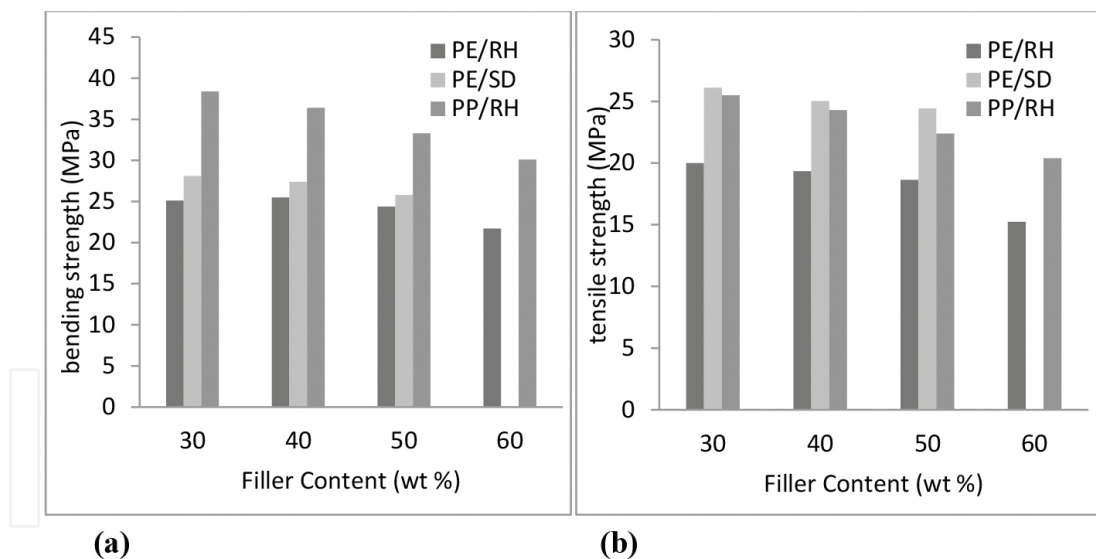


**Figure 5.** Effect of filler content on (a) bending strength (b) tensile strength of the composites, no compatibilizer added.

The addition of stiff fillers to the polyolefine matrices improves the stiffness of the composite, and the bending modulus increases linearly with filler content (**Figure 4**). The modulus reflects the capability of fiber and polymer matrix to transfer the elastic deformation in the case of small strains without interface fracture. The modulus of filled PP is 25% higher than that of both filled PEs. It is noted that at high content of saw dust (above 50 wt.%), the viscosity of melt compound is very high, leading to voids and reducing the modulus.

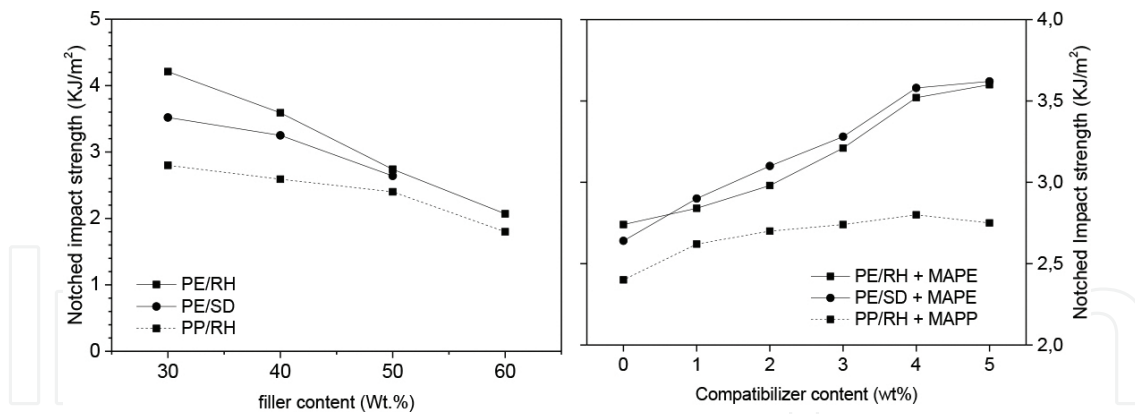


**Figure 6.** Left: Effect of filler content on impact strength of the composites, no compatibilizer added. Right: Influence of compatibilizer content on impact strength of the composites at 50% filler content.

The bending strengths (**Figure 5a**) are mainly influenced by the matrix type: PP/RH has 40% increased bending strength compared to the PE composites. Considering the volume filler content, the data for the bending strength of PE/RH and PE/SD coincide.

The saw dust/polyethylene composites show 20% higher tensile strengths compared to the rice husk/polyethylene composites (**Figure 5b**). This is probably caused by the higher cellulose content, better adhesion, and the higher aspect ratio of saw dust compared to the rice husk filler [12]. The tensile strength of the PP/RH composite is 20% higher than that of the PE/RH.

There is a clear decrease in tensile and bending strength in dependence on filler content throughout the investigated range. The fillers introduce a large interface area; in unmodified polymers, this is dominant due to weak interfacial interaction between the polar bio-filler and the apolar polyolefine matrix. As filler is added, this surface area increases, resulting in a slight decrease in the tensile, bending, and impact strengths of three composite systems PE/RH, PE/SD, and PP/RH in the absence of compatibilizer. The decrease is linear up to 50 wt.% (i.e., 46 vol.% of SD, 43 vol.% of RH) of filler. Specimens of 60 wt.% SD in PE could not be injection molded with the current set up, and samples of 60 wt.% RH in PE showed a stronger-than-linear decrease. At concentrations approaching the theoretical packing limit (e.g., 74 vol.% for oriented spherical rod fillers), defects and voids occur, the viscosity increases, and the weak, unbound interphase plays an increasing role.

**Figure 6** presents the notched Izod impact strengths of rice husk and saw dust composites. The impact strength of a composite is influenced by many factors, especially the toughness of the filler and matrix components, and the dynamic stress transfer of the interphase, which in turn is determined by particle size, shape, and filler surface properties [13–15]. The notched impact strength of RH/PE composites, **Figure 6a**, is better than that of SD/PE composites when no compatibilizer is added. The PP/RH composites show lower impact toughness than PE composites. This trend is similar to a polypropylene composite system published by Bledzki et al. [15], where it is attributed to the brittleness and local internal deformation found more commonly in wood composites. Particle size, shape, and filler surface properties have influence

on the impact strength [14]. The nature of the interphase plays an important role, and in the case of fibrous material, the frictional work involved in pulling the fibers out of the matrix.

A matrix modification was performed by using compatibilizers (MAPE for PE matrix composites and MAPP for PP matrix composites) in order to improve the bonding strength between the bio-fillers and the matrix polyolefine. **Figures 6b** and **7** show the effect of compatibilizer content on the impact strength of the composites containing 50 wt.% filler. Tensile, bending, and impact strengths increased while adding compatibilizer and leveled off at above 2 wt.% MAPP for PP matrix composites and at above 4 wt.% MAPE for PE matrix composites. The increase in strengths of the composites is due to the improved interfacial adhesion between the fillers and polyolefine matrices. The maleic anhydride groups of compatibilizer interact with the polar filler surface (through chemical coupling or hydrogen bonding), while their polyolefine chains diffuse into the polyolefine matrices. Therefore, the interfacial strength is improved, as seen before, for example, by Marti-Ferrer et al. and Correa et al. [4, 5]. The increase in tensile, bending, and impact strengths due to the compatibilizers is higher than the losses due to the inclusion of fillers.

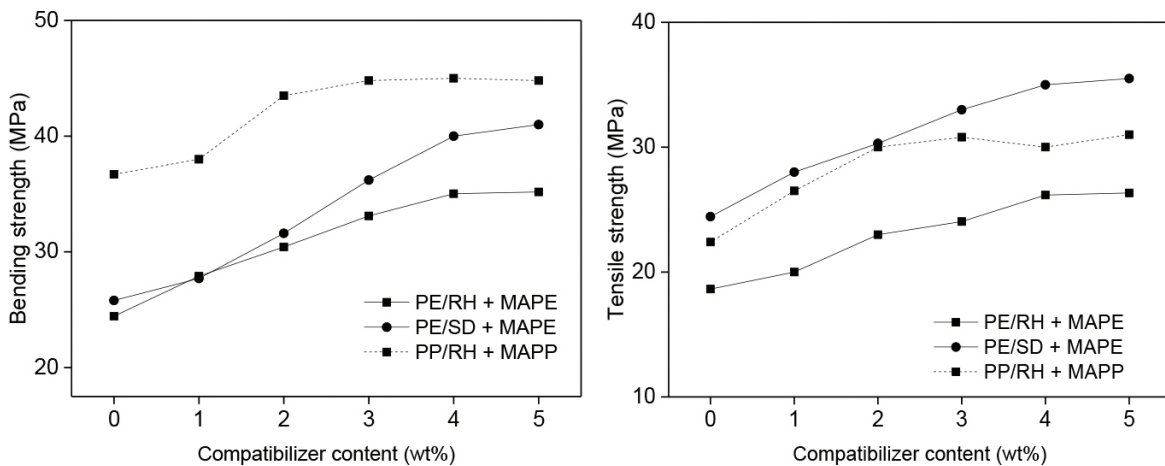


**Figure 7.** Influence of compatibilizer content on bending (left) and tensile strength (right) of the composites at 50% filler content.

### 3.3. Composite fracture surfaces and cross-sectional analysis

**Figure 8** shows SEM images of the tensile fracture surfaces of the composites at 50 wt.% filler without and with compatibilizers (2 wt.% MAPP for PP matrix composites and 4 wt.% MAPE for PE matrix composites). Adding the compatibilizers changes the fracture behavior of the composites. The unmodified composites fail at the interphases of the filler particles. Voids at the interphase (especially the outside surface of RH particles) and pull-out cavities (especially in the higher aspect ratio SD particles) are visible. In the modified composite, the interfacial interaction is improved, shifting the failure into the matrix with far less pull-out cavities and polymer-coated or partially coated filler particles.

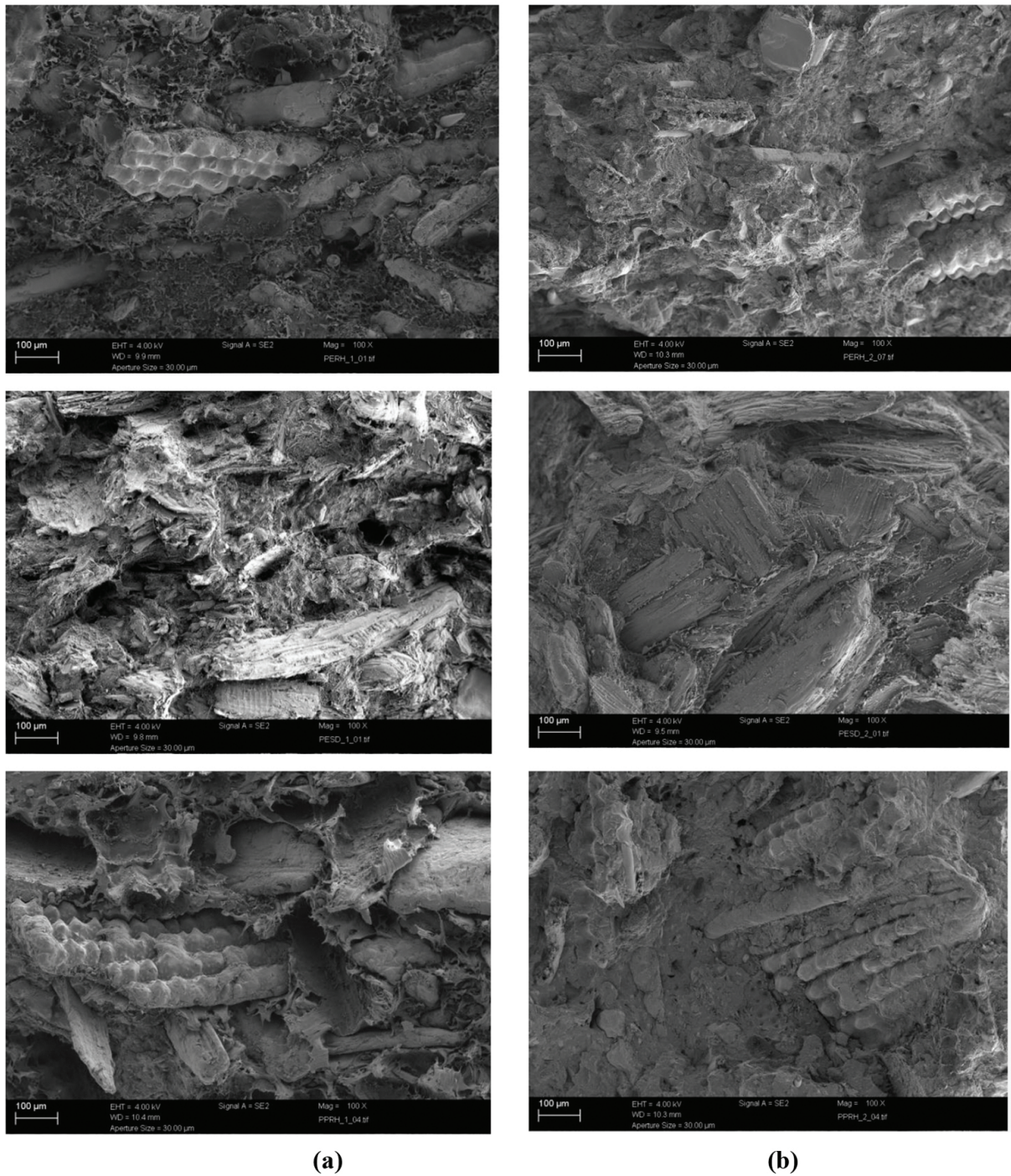


**Figure 8.** SEM micrographs of tensile fracture surfaces of PE/RH composites (top), PE/SD composites (middle), and PP/RH composites (bottom), (a) without and (b) with compatibilizer. Scale bar: 100 µm.

**Figure 9** shows SEM micrographs of polished cross-sections for the composites in the longitudinal and transverse specimen direction. The saw dust is oriented along the specimen long axis due to the injection molding process. Here, an anisotropic mechanical behavior is expected. In rice husk, no preferred orientation of the platelets is seen for either PP/RH (as **Figure 9** bottom) or PE/RH (not shown here).

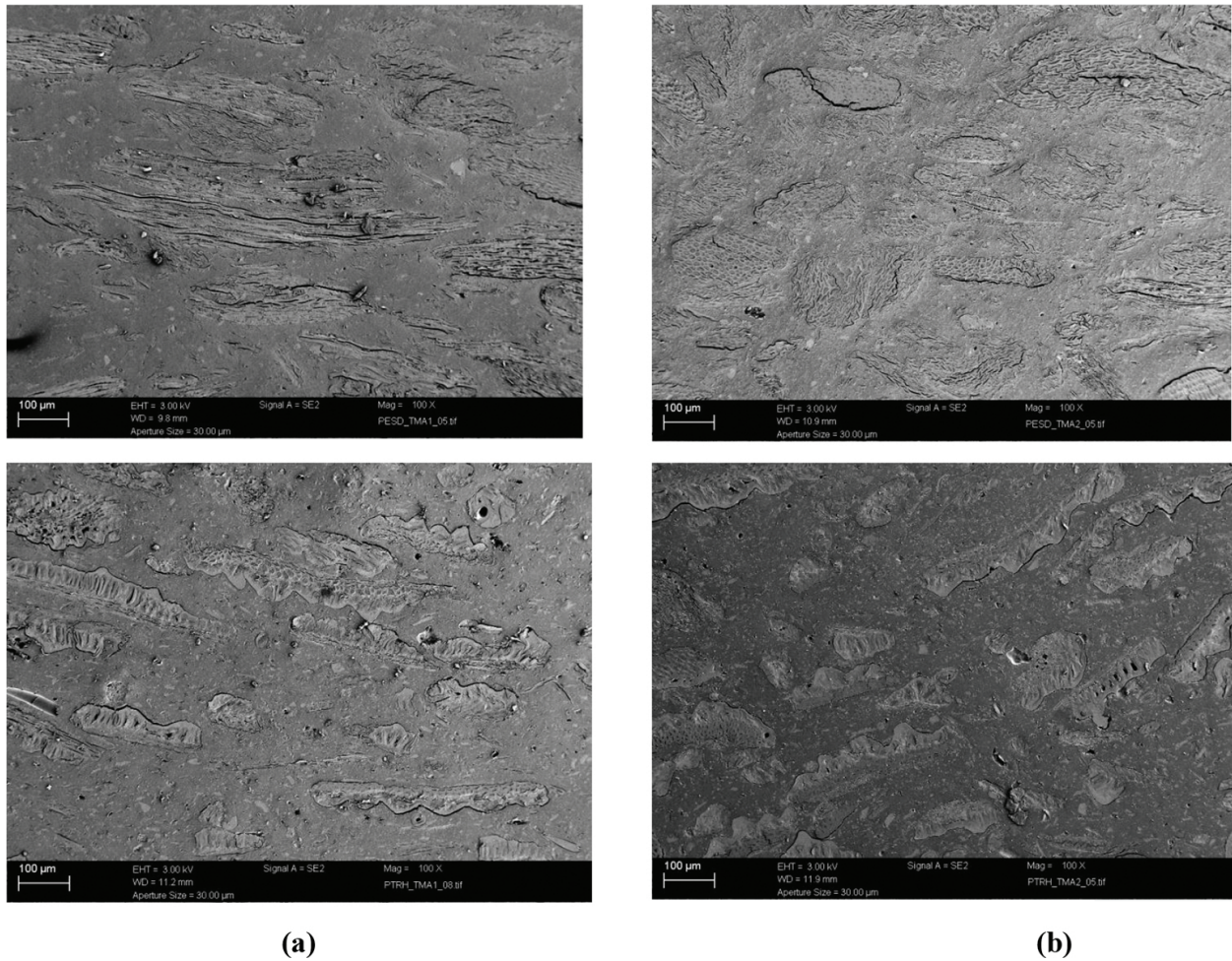


**Figure 9.** SEM photomicrographs of polished samples of PE/SD composites (top) and PP/RH composites (bottom), in x-direction (a) and in z-direction (b).

### 3.4. Hardness

**Figure 10** shows the effect of the fillers on the hardness of three modified matrix composites [PE/RH (MA), PE/SD (MA), and PP/RH (MA)]. The fillers increased the hardness of polyolefines significantly. Neat and filled polypropylene had a higher hardness than neat resp. filled polyethylene. The addition of 50 wt.% fillers improved significantly the hardness of three composite systems. The hardness of PE and PP matrix composites increased about 78 and 65%, respectively. This was expected, since the chosen bio-fillers display considerably higher hardness than the soft polyolefine matrices, the hardness of RH being higher than that of SD. Thus, it was also expected that for the PE composites, the hardness of the PE/RH composites would be higher than that of the PE/SD composite. In fact, they had the same value at 50 wt.% filler content. This result could be caused by the higher volume content of SD filler (43 vol.%) compared to that of RH (39 vol.%). The hardness values can be considered as a measure of the wear resistance, since hard materials resist friction and wear better [15].

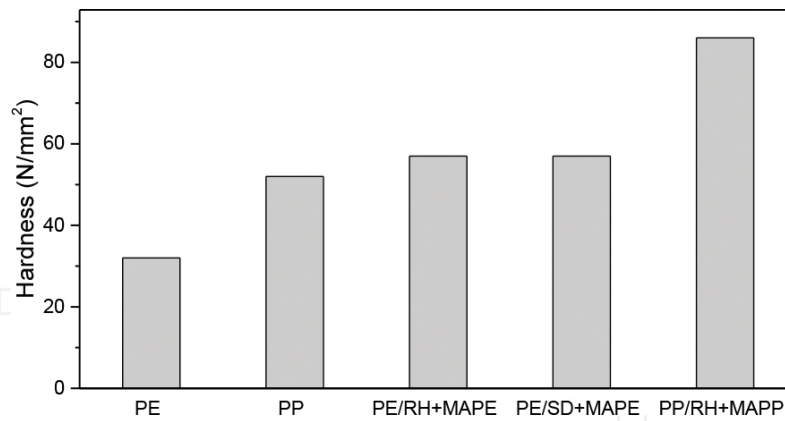


Figure 10. Hardness of polyolefine and filler/polyolefine composites at 50 wt.% filler content.

### 3.5. Thermomechanical analysis (TMA)

Figure 11 shows the thermal expansion as determined by TMA in x-direction and the coefficient of thermal expansion (CTE) values of the modified matrix composites [PE/RH (MA), PE/SD (MA), and PP/RH (MA)], respectively. The CTE values of pure PE and PP were determined to  $134 \times 10^{-6}/^{\circ}\text{C}$  and  $123 \times 10^{-6}/^{\circ}\text{C}$  for the temperature range of  $-10$  to  $50^{\circ}\text{C}$ , respectively. Thermal expansion is higher for the range  $50$ – $100^{\circ}\text{C}$  ( $210 \times 10^{-6}/^{\circ}\text{C}$  for PE and  $163 \times 10^{-6}/^{\circ}\text{C}$  for PP). CTE values of pure PE and PP decreased to 30–62% by adding 50 wt.% filler. While the CTE values of rice husk composites are isotropic, the difference in CTE values in longitudinal and transverse directions of the saw dust composite is quite high, especially in the high-temperature range  $50$ – $100^{\circ}\text{C}$  ( $94 \times 10^{-6}/^{\circ}\text{C}$  in x-direction and  $187 \times 10^{-6}/^{\circ}\text{C}$  in z-directions). This reflects on the one hand the anisotropic behavior of the saw dust [16] and on the other hand the aspect ratio of the SD particles which in injection molding lead to orientation of the filler particles, confer Figure 9.

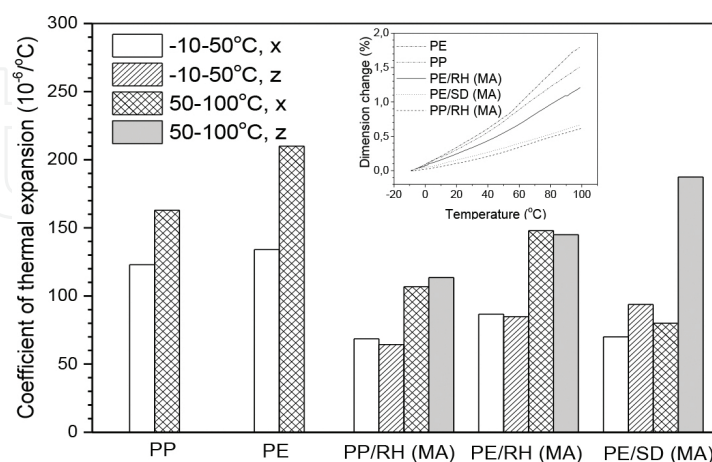
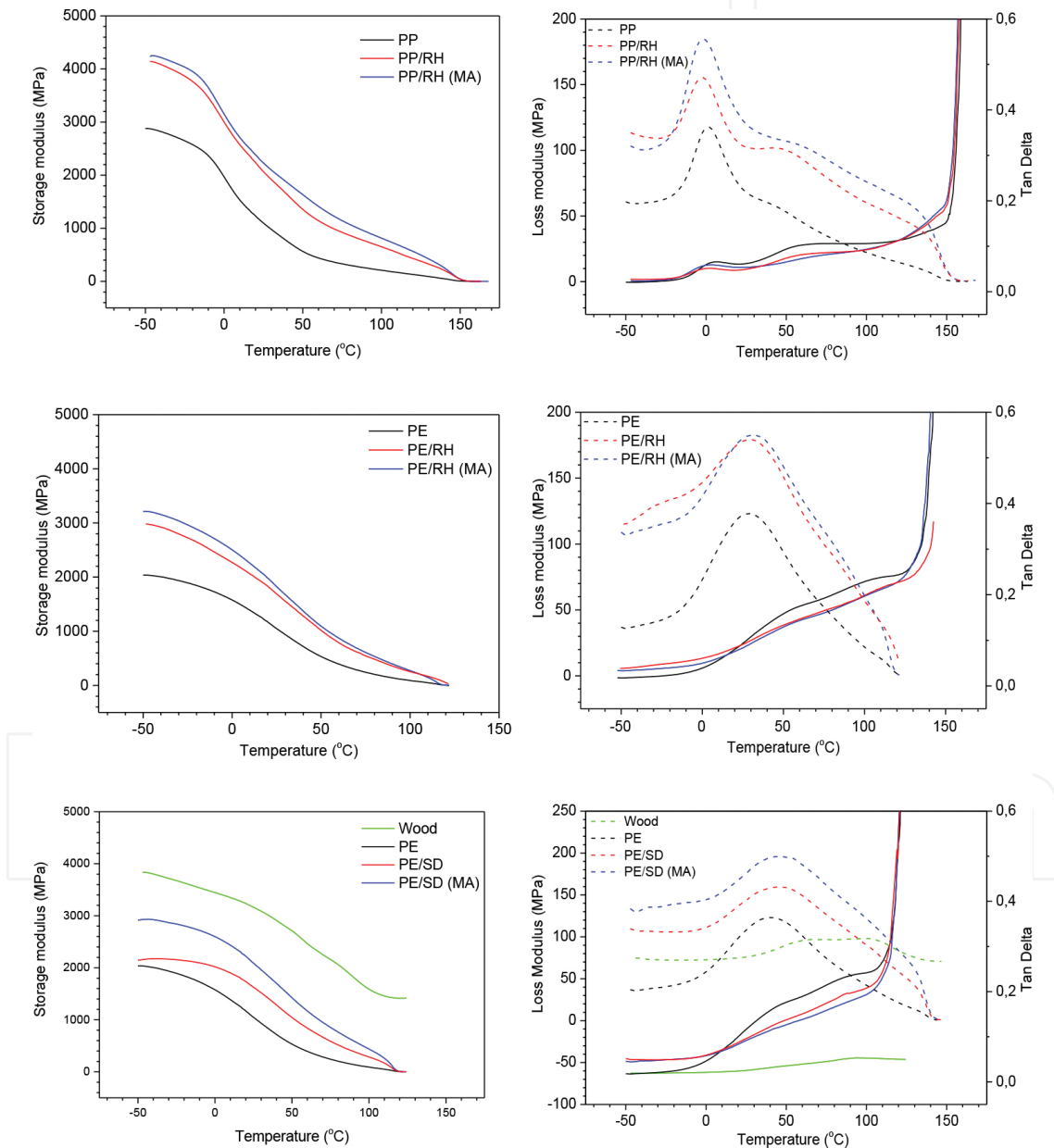


Figure 11. Coefficient of thermal expansion of polyolefine and filler/polyolefine composites. inset: Dimension change of polyolefine and filler/polyolefine composites in x-direction.

### 3.6. Dynamic mechanical thermal analysis (DMTA)

Dynamic mechanical thermal analysis (DMTA) is a sensitive technique that characterizes the mechanical responses of materials by monitoring property changes with respect to the temperature and/or frequency of oscillation [17]. It has been commonly used as a technique for investigating the viscoelastic behavior of the composites for determining their dynamic modulus such as storage modulus ( $E'$ ), viscous behavior (loss modulus  $E''$ ), and energy damping ( $\tan \delta$ ) as a function of temperature [18–19]. The elastic component describes the energy stored in the system, while the viscous part describes the energy dissipated.



**Figure 12.** DMTA: storage modulus (left), loss modulus, and  $\tan \delta$  (right) of PP, PE, wood, and composites with 50% filler loading, without and with compatibilizer.

**Figure 12** shows the storage modulus  $E'$ , the loss modulus  $E''$ , and  $\tan \delta$  values of the composites without and with compatibilizers as well as the stock materials PP, PE, and wood. The storage modulus ( $E'$ ) of polypropylene and polyethylene matrix composites was higher than those of pure polypropylene and polyethylene matrices, respectively. This is the expected effect caused by the addition of high surface rigid fillers into semi-rigid polyolefine matrices. In all the systems, the storage modulus drops with increasing temperature due to the increased segmental mobility of the polymer chains. The  $E'$  value of polypropylene systems decreased rapidly at the glass transition above  $0^\circ\text{C}$ , whereas the  $E'$  value of wood and polyethylene systems decreased in a wider range around  $30^\circ\text{C}$ .

The temperature dependence of loss modulus and  $\tan \delta$  for the polyolefine, wood, and three composite systems without and with compatibilizers is presented in **Figure 12**. The loss modulus ( $E''$ ) is a measure of the absorbed energy due to the relaxation and is associated with viscous response of the viscoelastic materials.  $E''$  of polyolefine and composites increased with temperature and had a peak in the transition region about 0 and  $30^\circ\text{C}$  for PP and PE systems, respectively.

The damping factor  $\tan \delta$ , defined as the ratio of the loss modulus to the storage modulus ( $E''/E'$ ), is commonly used to characterize viscoelastic behavior of the materials, for example,  $T_g$  and energy dissipation of composite materials. With increasing temperature, the  $\tan \delta$  values of PP and PP matrix composites increased due to the increased polymer chain mobility of the matrix and exhibited two relaxation peaks in the vicinity of 5 and  $70^\circ\text{C}$ . The low-temperature peak is related to the glass transition of the amorphous polymer fractions [20–21]. The high-temperature peak corresponds to the  $\alpha$  transition related to the PP crystalline fractions. The  $\alpha$  transition peak of the modified PP composite ( $81^\circ\text{C}$ ) was higher than that of the unmodified one ( $72^\circ\text{C}$ ) that can be a result of the existence of enhanced transcrystallinity around the fibers in the modified composites [20, 22].

For the polyethylene system,  $\tan \delta$  curves of neat PE and the composites had less distinctive  $\alpha$  transition processes compared to the loss modulus curves and there was no peak corresponding to the  $T_g$  of polyethylene (approximately  $-130^\circ\text{C}$ ) because it was not sufficiently cooled down to this temperature while carrying out the test. The  $\alpha$  relaxation is generally attributed to segmental motions in the noncrystalline phase [23]. The  $\alpha$  transition of the composites shifted to higher temperature compared to neat polyolefine. An addition of compatibilizer also led to shift slightly the  $\alpha$  transition curve to the higher temperature, that is an indication of the presence of some processes, which have restricted the mobility of the chains in the crystalline phase so that more energy is required for the transition to happen. Therefore, the natural fibers somehow restricted the matrix polymer chains and increased the  $\alpha$  transition temperature [17].

### 3.7. Differential scanning calorimetry (DSC) analysis

Differential scanning calorimetry (DSC) can be used to measure melting temperature ( $T_m$ ), crystallization temperature ( $T_c$ ), and crystalline content ( $X_c$ ) of materials. **Figure 13** presents the heating and cooling thermograms for neat matrices and modified polyolefine composites which contain 50 wt.% fillers. The  $T_m$  of neat matrices and the composites was obtained from

the maximum of the endothermic melting peak (heating curves). The  $T_m$  of polyolefines was not significantly changed by the addition of bio-fillers. The peak area is reduced by 50% due to the filler, as expected.

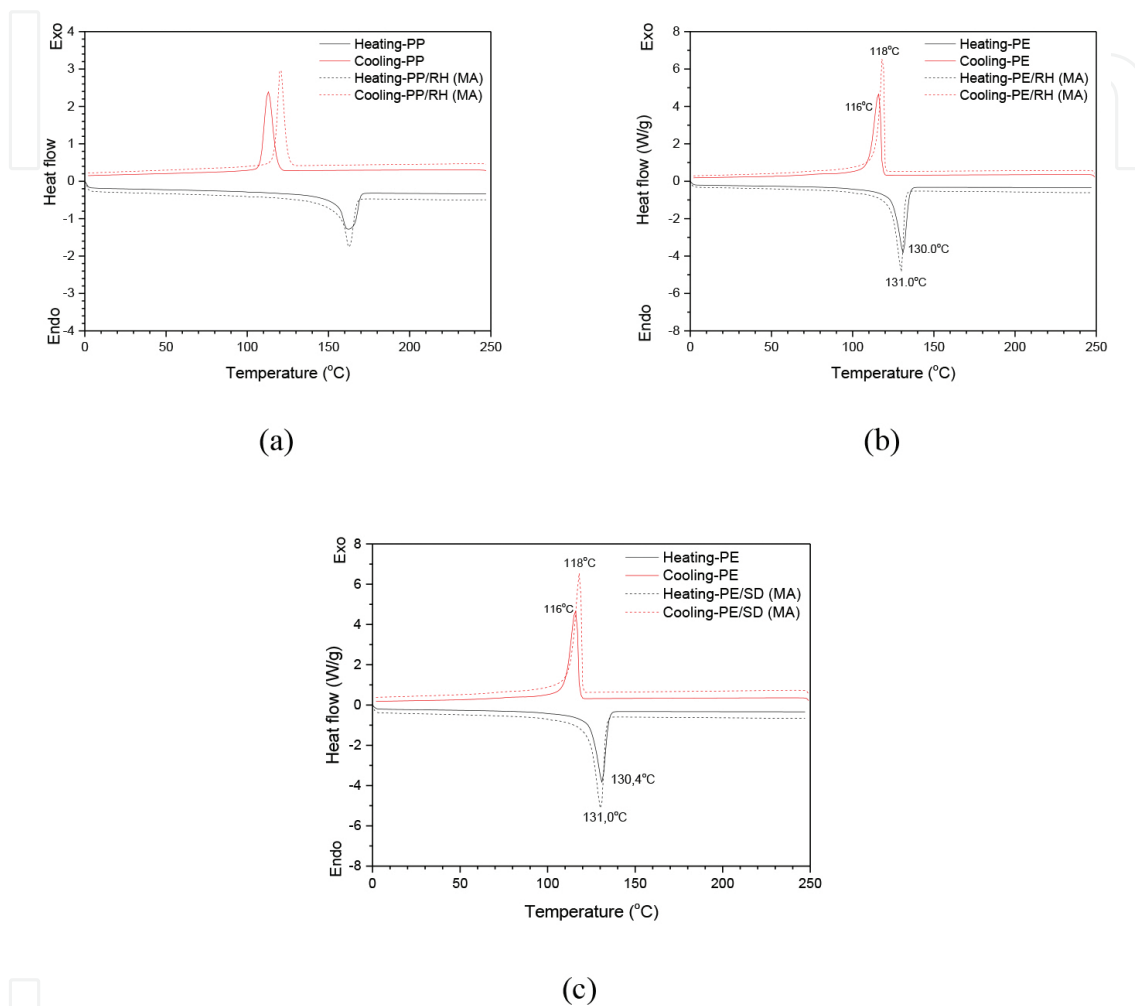


**Figure 13.** DSC heating (2nd run) and cooling curves of neat matrix and modified composites (50% filler) of (a) PP/RH, (b) PE/RH, and (c) PE/SD without and with compatibilizer.

To characterize the polyolefine crystallization, the crystallization peaks of the cooling run were analyzed, confer **Table 2**.  $T_c$  of neat matrices and the composites was obtained from the maximum of the exothermic crystallization peak. The crystallization is influenced by the fillers: For PP matrix without filler, the crystallization peak was observed at  $T_c = 113^\circ\text{C}$ , while for the PP matrix composites, these exothermic peaks shifted to higher temperatures ( $T_c = 120^\circ\text{C}$ ).

This shift to earlier crystallization in the cooling run is due to the nucleating ability of the compatibilizer MAPP, which is enriched in the interphase, and perhaps the cellulosic filler surface, creating a transcrystalline interphase morphology, which improves the material properties [24].

The  $T_c$  of polyethylene systems ( $T_c = 116^\circ\text{C}$ ) does not increase significantly upon addition of the fillers ( $T_c = 118^\circ\text{C}$ ). As the neat PE crystallizes only  $10^\circ\text{C}$  below  $T_m$  and PE is a fast crystallizing thermoplast (i.e., the width of the crystallization peak is narrow), nucleation influences  $T_c$  less than in PP, where the difference  $T_m - T_c = 30^\circ\text{C}$ .

Samples	$T_m$ ( $^\circ\text{C}$ )	$T_c$ ( $^\circ\text{C}$ )	$T_c$ ( $^\circ\text{C}$ ) (onset)
PP	162.2	112.9	118.3
PP/RH (MA)	162.7	120.5	124.6
PE	131.0	115.9	118.1
PE/RH (MA)	130.0	118.5	119.6
PE/SD (MA)	130.4	118.2	119.7

**Table 2.** Thermal properties determined by DSC.

### 3.8. Thermogravimetric analysis (TGA)

Thermogravimetric analysis is becoming an increasingly useful tool for material characterization, particularly in the development of new materials. It is essential to monitor not only the final properties of the composites but also the basic raw materials through the processing procedure to the final product. Optimization of the processing temperature and time with an understanding of matrix, reinforcing element and interface between matrix and reinforcing phase, can lead to the best balance of composite properties such as modulus, thermal stability, and damping behavior [25]. Thermogravimetric analysis (TGA) can determine the moisture content, thermal cleavage, thermal degradation temperature, and thermal stability of composite materials [26, 27]. The differential thermogravimetric analysis (DTG) i.e. the slope of the TGA data curve, permits a more detailed analysis of thermal decomposition.

#### 3.8.1. Fillers and Polyolefines

**Figure 14** shows the results of the thermal analysis of the used polyolefines and fillers performed in nitrogen and air atmosphere. The TGA and DTG curves of the fillers in nitrogen as well as air atmosphere show a slight weight loss between  $40$  and  $100^\circ\text{C}$ , indicating the vaporization of water. A second weight loss from approximately  $150$ – $500^\circ\text{C}$  is due to the decomposition of the three major constituents of bio-fillers, namely cellulose ( $275$ – $350^\circ\text{C}$ ), hemicellulose ( $150$ – $350^\circ\text{C}$ ), and lignin ( $250$ – $500^\circ\text{C}$ ) [26, 28–30]. At  $700^\circ\text{C}$ , rice husk and saw dust leave a greater char content, decomposing only by about 65 and 80% in nitrogen cf. **Table 3**. The ash in the RH is mainly composed of silica (96%) [26]. In an air atmosphere, rice husk degradation shifted to lower temperature values and split into two processes ( $320$  and  $438^\circ\text{C}$ ). The second may be associated with thermal oxidation degradation of char. Therefore, the residues of RH filler at  $700^\circ\text{C}$  in the air atmosphere (20%) were lower than that in nitrogen atmosphere (36%).

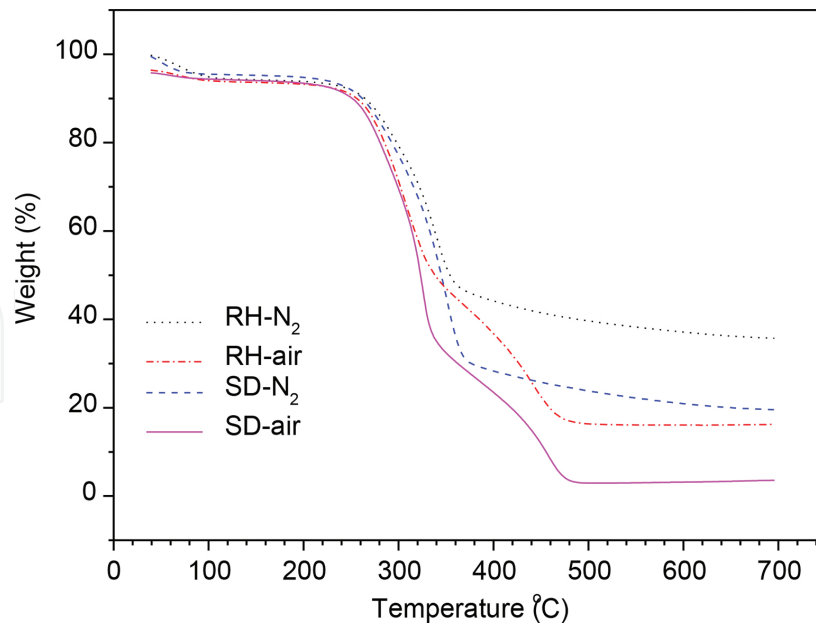


**Figure 14.** TGA curves of stock materials: fillers saw dust and rice husk as well as polyolefines PP and PE in nitrogen and air atmospheres.

	Residue in nitrogen atmosphere			Residue in air atmosphere		
PP	1.8			0.8		
PE	1.8			1.0		
RH	35.7			19.8		
SD	19.6			7.8		
<i>Filler content</i>	30%	40%	50%	30%	40%	50%
PP/RH	11.0	12.7	14.1	5.5	6.9	8.0
PE/RH	10.9	12.2	18.8	5.5	6.7	9.4
PE/SD	4.5	7.4	8.8	1.0	1.0	1.3

**Table 3.** Residues of polymers and fillers as well as their composites at 700°C in nitrogen and air atmosphere in %.

PE and PP decompose at temperatures above 400°C, cf. **Figure 14**. In nitrogen atmosphere, thermal degradation of PP and PE occurs very rapidly at 468 and 488°C, respectively. In air, the thermal resistance of both polyolefines (PP and PE) starts at 250°C. While PP is fully degraded at 380°C, PE decomposed more gradually and is fully degraded at 470°C. The maximum decomposition rates of PP and PE in the air occurred at 371 and 399°C, respectively. Both PP and PE decomposed almost completely. Residues of both polyolefines at 700°C were <2% in nitrogen and <1% in air atmosphere.

### 3.8.2. Composites

**Figure 15** shows the TGA and DTG curves of the polyolefines, fillers, and the composites with filler content ranging from 30 to 50 wt.% in nitrogen and air atmosphere. The TGA or DTG

analyses performed in nitrogen atmosphere show two regions of thermal decomposition that consist of the superposition of the profiles of filler and polyolefines. As the filler is less thermally stable than the matrix polymer, when filler loading is increased, the thermal stability of the composites slightly decreases, whereas the final ash content increased (**Table 3**).

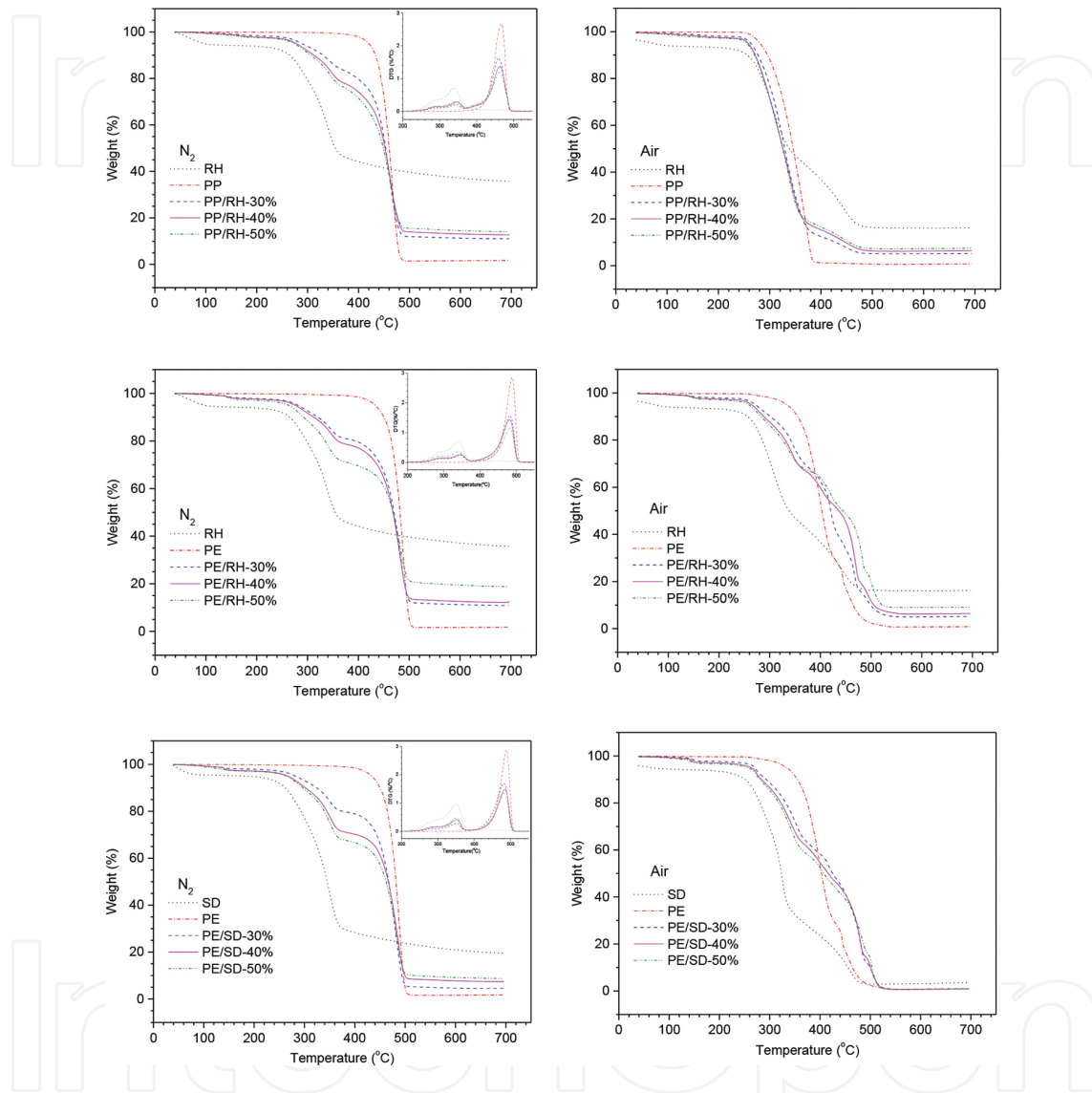


**Figure 15.** TGA of fillers, plastics, and the composites in nitrogen (left) and air (right) of PP/RH (top), PE/RH (middle), and PE/SD (bottom) composites, inset in left images: DTG.

In the case of the two studied PE composites decomposed in air, the TGA/DTG curves of the composites correspond to the superposition of the separate components only up to 400°C, whereas the charring behavior is different. The final reduction is only reached at 500°C, 60°C above the temperature where both PE and filler are completely degraded thermally. That may be due to a thermally stable material (char), formed during the oxidation or thermal degradation of hemicellulose, cellulose, and lignin, providing a thermal shielding and acting as diffusion barrier on the polyethylene decomposition process. Moreover, the second

peak of decomposition of olefinic products or their oxidation degradation products containing functional groups such as C=O, O–H, and C–O–C which formed in the first stage of polyethylene degradation appears at 438°C. This second main peak of PE degradation is in superposition with the second main peak of the bio-fillers due to degradation of char (**Figure 15a**). Therefore, the second-stage degradation of both polyethylene and the bio-fillers is competitive at above 438°C, that can also lead to retard the degradation of the composite. However, there is a one-step degradation of polypropylene in air atmosphere and PP fully degraded at 380°C. Therefore, RH char did not affect the degradation of polypropylene.

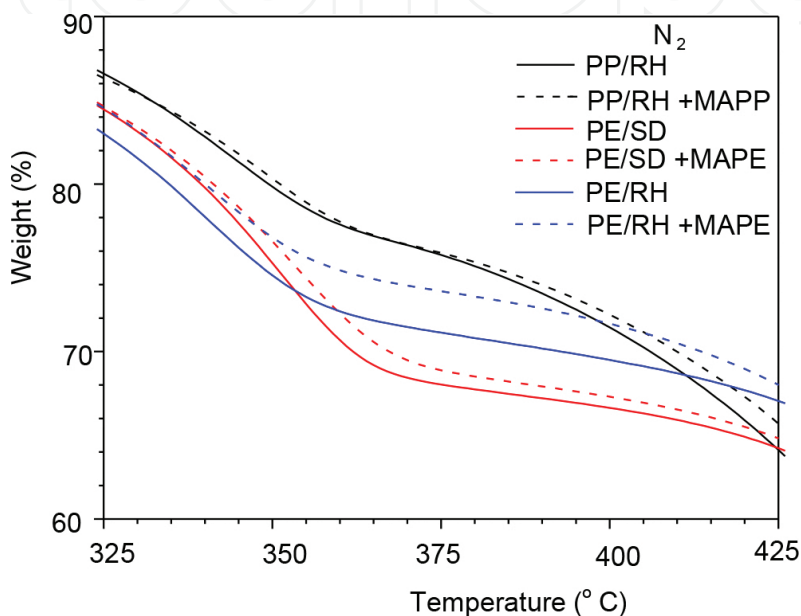


**Figure 16.** Effect of compatibilizers on TGA of 50% filler composites in nitrogen atmosphere.

The RH-filled PE leaves a bigger residue than the SD-filled PE, as expected from the TGA analysis of the fillers. The residues of rice husk composites (10.9–18.8% in nitrogen and 5.5–9.4% in air atmosphere) were much higher than those of saw dust composites (4.5–8.8% in nitrogen and 1.0–1.3% in air atmosphere) due to high ash content of rice husk compared to saw dust. The residue is in all cases 0–10% smaller than the value calculated from the residues of the separate components, and only in the saw dust composites in air, it is a third of the expected value. The filler/matrix interaction leads to a more profound decomposition maybe due to a wick effect.

**Figure 16** shows the TGA curves of the composites at 50 wt.% filler without and with compatibilizers (2 wt.% for PP matrix composites and 4 wt.% for PE matrix composites). The thermal stability and degradation temperature of the composites with compatibilizers [PP/RH (MA), PE/RH (MA), and PE/SD (MA)] were slightly higher than those of the composites without compatibilizers (PP/RH, PE/RH, and PE/SD). The improved thermal stability of the composites with compatibilizers is due to enhanced interfacial interaction and additional intermolecular bonding (ester and hydrogen bonds) between hydroxyl groups of rice husk, saw dust and the anhydride functional groups of compatibilizers.

## 4. Conclusions

The performance of rice husk and saw dust fillers, used as low ecological footprint reinforcement of PE and PP, was investigated. SEM micrographs show the different morphology of rice husk platelets and fibrous saw dust fillers. Rice husk has the higher stiffness and the higher density of the two fillers considered. In a PE or PP matrix, the fillers increase the bending moduli. In composites without compatibilizer, an increase in filler load leads to decreased tensile, bending, and impact strengths.

Here, PE matrix composites with saw dust have smaller moduli but higher strengths than those with rice husk filler. The tensile, bending, and impact strengths of bio-filler/polyolefine composites increase with increasing compatibilizer content, due to the improvement in interfacial bonding strength between filler and matrix. The coefficient of thermal expansion of PP and PE decreased upon adding rice husk and saw dust fillers.

The thermal stability of the fillers or natural fibers in general is not as high as that of high-performance fibers. This limits the matrices of thermoplastic composites with bio-fillers to those materials processable below 200°C, such as PP, PE, or polylactic acid (PLA).

Rice husk and saw dust can be used as fillers in manufacturing inexpensive polyolefine composites for furniture and household articles as well as construction materials, generating economic development for rural areas and reducing environmental pollution caused by these bio-wastes if unused.

## Acknowledgements

The authors are thankful to Chemtura Company for supplying the materials; Dr. Jianwen Liu, Sabine Krause, Birgit Schulze, Liane Häussler, Thanh Tran, Hang Tran, Dung Pham, Hieu Nguyen, Dat Nguyen, Xuan Vo, Linh Nguyen, Quang Le, Huan Vo, Chuong Hien, Men Tran, Truong Le, Huan Le, Nghia Tran, and Linh Pham for experimental assistance.

## Author details

Thi Thu Loan Doan<sup>1</sup>, Hanna M. Brodowsky<sup>2\*</sup> and Edith Mäder<sup>2</sup>

\*Address all correspondence to: [brodowsky@ipfdd.de](mailto:brodowsky@ipfdd.de)

<sup>1</sup> Danang University of Science and Technology, Department of Chemical and Material Engineering, Danang, Vietnam

<sup>2</sup> Leibniz-Institut für Polymerforschung e.V., Department of Composite Materials, Dresden, Germany

## References

- [1] Faruk O, Bledzki AK, Fink HP, Sain M. Biocomposites reinforced with natural fibres: 2000–2010. *Progr. Polym. Sci.* 2012; 37:1552-1596. doi: 10.1016/j.progpolymsci.2012.04.003
- [2] Yao F, Wu Q, Lei Y, Xu Y. Rice straw fibre-reinforced high-density polyethylene composite: effect of fiber type and loading. *Ind. Crops Prod.* 2008;28(1):63–72. doi: 10.1016/j.indcrop.2008.01.007
- [3] Panthapulakkal S, Sain M, Law S, Effect of coupling agents on rice-husk-filled HDPE extruded profiles. *Polym. Int.* 2005;54:137–142. doi: 10.1002/pi.1657
- [4] Marti-Ferrer F, Vilaplana F, Ribes-Greus A, Benedito-Borras A, Sanz-Box C. Flour rice husk as filler in block copolymer polypropylene: effect of different coupling agents. *J. Appl. Polym. Sci.* 2006; 99:1823–1831. doi: 10.1002/app.22717
- [5] Correa CA, Razzino C, Hage E. Role of maleated coupling agents on the interface adhesion of polypropylene-wood composites. *J. Thermoplast. Compos. Mater.* 2007;20:323–339. doi: 10.1177/0892705707078896
- [6] Keener TJ, Stuart RK, Brown TK. Maleated coupling agents for natural fibre composites. *Composites A.* 2004;35:357–362. doi: 10.1016/j.compositesa.2003.09.014
- [7] Doan TLL, Gao SL, Mäder E. Jute/polypropylene composites I. Effect of matrix modification. *Compos. Sci. Technol.* 2006;66:952–963. doi: 10.1016/j.compscitech.2005.08.009
- [8] Doan TTL, Brodowsky HM, Mäder E. Jute fibre/ polypropylene composites II. Thermal, hydrothermal and dynamic mechanical behaviour. *Compos. Sci. Technol.* 2007;67(13): 2707–2714. doi:10.1016/j.compscitech.2007.02.011
- [9] Negri AP, Cornell HJ, Rivett DE. A model for the surface properties of fibers. *J. Text. Res.* 1992;63:109–16.
- [10] Essabir H, Hilali E, ElGharad A, El Minor H, Imad A, Elamraoui A, Al Gaoudi O. Mechanical and thermal properties of bio-composites based on polypropylene reinforced with nut shells of Argan particles. *Mater. Des.* 2013;49:442–448. doi: 10.1016/j.matdes.2013.01.025
- [11] Fu SY, Feng XQ, Lauke B, Mai YW. Effects of particle size, particle/matrix interface adhesion and particle loading on mechanical properties of particulate–polymer composites. *Composites B* 2008;39:933–61. doi: 10.1016/j.compositesb.2008.01.002
- [12] Yao F, Wu Q, Lei Y, Xu Y. Rice straw fiber-reinforced high-density polyethylene composite: effect of fiber type and loading. *Ind. Crops Prod.* 2008;28(1):63–72. doi: 10.1016/j.indcrop.2008.01.007

- [13] Bledzki AK, Mamun AA, Volk, J. Barley husk and coconut shell reinforced polypropylene composites: the effect of fibre physical, chemical and surface properties. *Compos. Sci. Technol.* 2010;70:840–846. doi: 10.1016/j.compscitech.2010.01.022
- [14] Bledzki AK, Mamun AA, Volk J. Physical, chemical and surface properties of wheat husk, rye husk and soft wood and their polypropylene composites. *Composites A* 2010;41:480–488. doi: 10.1016/j.compositesa.2009.12.004
- [15] Bledzki AK, Mamun AA, Bonnia NN, Ahmad S. Basic properties of grain by-products and their viability in polypropylene composites. *Ind. Crops Prod.* 2012;37:427–434. doi: 10.1016/j.indcrop.2011.05.010
- [16] Lee SM, Cho D, Park WH, Lee SG, Han SO, Drzal LT. Novel silk/poly(butylene succinate) biocomposites: the effect of short fibre content on their mechanical and thermal properties. *Compos. Sci. Technol.* 2005;65:647–657. doi: 10.1016/j.compscitech.2004.09.023
- [17] Behzad M, Tajvidi M, Ehrahimi G, Falk RH. Dynamic mechanical analysis of compatibilizer effect on the mechanical properties of wood flour/high-density polyethylene composites. *IJE Trans. B* 2004;17:95–104.
- [18] Lopez-Manchado MA, Arroyo M. Thermal and dynamic mechanical properties of polypropylene and short organic fibre composites. *Polymer* 2000;41:7761–7767. doi: 10.1016/S0032-3861(00)00152-X
- [19] Ray D, Sarkar BK, Das S, Rana AK. Dynamic mechanical and thermal analysis of vinyl ester-resin-matrix composites reinforced with untreated and alkali-treated jute fibres. *Compos. Sci. Technol.* 2002;62:911–917. doi: 10.1016/S0266-3538(02)00005-2
- [20] Amash A, Zugenmaier P. Study on cellulose and xylan filled polypropylene composites. *Polym. Bull.* 1998;40: 251-258. doi: 10.1007/s002890050249
- [21] Garcia-Martinez JM, Laguna O, Areso S, Collar EP. A dynamic–mechanical study of the role of succinyl-fluoresceine grafted atactic polypropylene as interfacial modifier in polypropylene/talc composites.: Effect of grafting degree. *Eur. Polym. J.* 2002; 38:1583-1589. doi: 10.1016/S0014-3057(02)00051-4
- [22] Quan H, Li ZM, Yang MB, Zhang R. On transcrystallinity in semi-crystalline polymer composites. *Compos. Sci. Technol.* 2005; 65:999-1021. doi: 10.1016/j.compscitech.2004.11.015
- [23] Sirotkin RO, Brooks NW, The dynamic mechanical relaxation behavior of polyethylene copolymers cast from solution. *Polymer* 2001;42 :9801-9808. doi: 10.1016/S0032-3861(01)00535-3
- [24] Na K, Park HS, Won HY, Lee JK, Lee KH, Nam JY, Jin BS. SALS study on transcrystallization and fiber orientation in glass fiber/polypropylene composites. *Macromol. Res.* 2006;14:499-503. doi: 10.1007/BF03218715

- [25] George J, Bhagawan SS, Thomas S. Thermogravimetric and dynamic mechanical analysis of pineapple fibre reinforced polyethylene composites. *J. Therm. Anal.* 1996;47: 1121-1140. doi: 10.1007/BF01979452
- [26] Kim HS, Yang HS, Kim HJ, Lee BJ, Hwang TS. Thermal properties of agro-flour-filled biodegradable polymer bio-composites. *J. Therm. Anal. Cal.* 2005;81:299. doi: 10.1007/s10973-005-0782-7.
- [27] Mohanty S, Verma SK, Nayak SK. Compos. Dynamic mechanical and thermal properties of MAPE treated jute/HDPE. *Composites. Sci. Technol.* 2006;3/4:538-547. doi: 10.1016/j.compscitech.2005.06.014
- [28] Marcovich NE, Villar MA. Thermal and mechanical characterization of linear low-density polyethylene/wood flour composites. *J. Appl. Polym. Sci.* 2003;90:2775-2784. doi: 10.1002/app.12934
- [29] Wielage B, Lampke T, Marx G, Nestler K, Starke D. Thermogravimetric and differential scanning calorimetric analysis of natural fibres and polypropylene. *Thermochim. Acta* 1999;337:169-177. doi:10.1016/S0040-6031(99)00161-6
- [30] Hatakeyama H, Tanamachi N, Matsumura H, Hirose S, Hatakeyama T. Bio-based polyurethane composite foams with inorganic fillers studied by thermogravimetry. *Thermochim. Acta* 2005;431:155-161. doi:10.1016/j.tca.2005.01.065